Carbohydrate Polymers 80 (2010) 954–961

Contents lists available at ScienceDirect

Carbohydrate Polymers

journal homepage: www.elsevier.com/locate/carbpol

Characterization of asymmetric membranes of cellulose acetate from biomass: Newspaper and mango seed

Carla da Silva Meireles [a], Guimes Rodrigues Filho [a,*], Moacir Fernandes Ferreira Jr. [a], Daniel Alves Cerqueira [b], Rosana Maria Nascimento Assunção [c], Elaine Angélica Mundim Ribeiro [a], Patricia Poletto [d], Mara Zeni [d]

[a] *Laboratório de Reciclagem de Polímeros, Instituto de Química, Universidade Federal de Uberlândia (UFU), Campus Santa Mônica, Av. João Naves de Ávila, 2121, 38.400-902, Caixa Postal 593, Uberlândia-MG, Brazil*

[b] *Instituto de Ciências Ambientais e Desenvolvimento Sustentável, Universidade Federal da Bahia (ICADS/UFBA), Barreira-BA, Brazil*

[c] *Faculdade de Ciências Integradas do Pontal (FACIP/UFU), Campus do Pontal, Ituiutaba-MG, Brazil*

[d] *Departamento de Física e Química, Universidade de Caxias do Sul (UCS), Caxias do Sul-RS, Brazil*

ARTICLE INFO

Article history:
Received 17 September 2009
Received in revised form 22 December 2009
Accepted 7 January 2010
Available online 11 January 2010

Keywords:
Mango seed
Newspaper
Cellulose acetate
Asymmetric membranes

ABSTRACT

Asymmetric membranes may be used in a broad range of applications such as reverse osmosis, hemodialysis and separation of organic mixtures. In this paper, asymmetric membranes were produced using cellulose acetate (CA) from biomass: newspaper and mango seed. The degree of substitution of CA was 2.65 ± 0.07. Different formulations were used to prepare the CA membranes: CA/dichloromethane/water with and without magnesium perchlorate. The asymmetry of the membranes was characterized by scanning electron microscopy (SEM). Membranes produced with magnesium perchlorate presented higher water vapor flux than those produced without this salt. This difference is due to pore formation in the membrane skin when using magnesium perchlorate. Membrane substructure showed to be a determining factor in ion diffusion experiments. The coefficient of ion diffusion for the membrane of cellulose acetate from mango seed was $1.82 \times 10^{-8}\ cm^2\ s^{-1}$ while for the membrane of cellulose acetate from newspaper was $7.43 \times 10^{-8}\ cm^2\ s^{-1}$ which similar to the value reported in the literature for commercial CA ($8.46 \times 10^{-8}\ cm^2\ s^{-1}$).

1. Introduction

Cellulose acetate is usually produced from wood pulp, but alternative sources of cellulose have been explored and, in this sense, the Group of Polymer Recycling of the Federal University of Uberlândia has shown the viability of utilizing residues such as sugarcane bagasse (Rodrigues Filho, Cerqueira, Assunção, Meireles, & Valente, 2008a) and newspaper (Rodrigues Filho et al., 2008b) for producing cellulosic derivatives such as cellulose acetate (CA) and methylcellulose.

Mango seed is an abundant residue discarded by the industry of mango juice and its amount is increasing due to the expansion of fruit production. Brazil produces 1.3 million metric tons of mangoes a year, which are processed mostly as juice. The seeds correspond to 30–45% of the mango weight, depending on the variety, and remain as residue, which is usually burned or discarded. Therefore, alternatives for the use of this residue are necessary since most of the articles related to mango concern topics such as: (i) the quality and characterization of the fruit pulp (Olle, Lozano, & Brillouet, 1996); (ii) use the industrial residues such as byproducts of the juice extraction, seeds and peel for the extraction of bioactive compounds (enzymes, phenolic compounds, carotenoids, vitamins pectin) (Ajila, Bhat, & Rao, 2007); and (iii) use of the starch present in the mango seed for producing glucose (Velan, Krishnan, & Lakshmanan, 1995). The seed is formed by an external hard layer called integument and an inner embryo (Borges, Siqueira, Dias, & Cardoso, 1999). In this work, in order to use mango seeds, the inner part was discarded and the integument, which is mainly composed by cellulose, lignin and hemicelluloses, was characterized and utilized as source of cellulose. The seeds were from *Mangifera indica L.*, the Tommy Atkins variety.

Another important cellulose source in urban residue is newspaper. Brazilian paper production reached 9.2 million of metric tons in 2008, 140 thousand metric tons of which corresponds to press paper, which is used for printing newspaper. Press paper is produced from a conifer of the genus *Pinus*. The chemical composition of the wood pulp when producing press paper is not altered during the pulping process, which is either mechanical or thermomechanical, preserving high lignin and hemicellulose content. These components have influence in the derivatization process and, therefore, it is important to know the composition of the raw material to be used.

In this work, cellulose from newspaper and mango seeds were used as cellulose sources for producing CA asymmetric membranes. There are in the literature several articles concerning the

---

* Corresponding author. Tel.: +55 (34) 3239 4174x201; fax: +55 3239 4208.
E-mail addresses: guimes@ufu.br, guimes.rodriguesfilho@gmail.com (G.R. Filho).

0144-8617/$ - see front matter © 2010 Elsevier Ltd. All rights reserved.
doi:10.1016/j.carbpol.2010.01.012

application of CA membranes in separation processes (Chou, Yu, Yang, & Jou, 2007; Sossna, Hollas, Schaper, & Scheper, 2007). The use of these membranes is related not only to its chemical structure, but also to its morphology, which changes according to the preparation process. Considering the processing, membranes can be classified as dense or porous. These can also be classified as symmetric or asymmetric, depending on the existence or not of a homogeneous structure throughout the membrane thickness (Habert, Borges, & Nobrega, 2006). Asymmetric membranes present a skin, which is responsible for the separation, and a porous substructure, which usually works as mechanical support. These membranes are often produced by phase inversion with partial solvent evaporation and immersion in a coagulation bath. Swelling agents, such as salts and water, can be added to the polymeric solution and act as pore formers (Khulbe et al., 2001). The characteristics of these membranes can be controlled by the preparation methodology and define their application among which are reverse osmosis (water desalination), hemodialysis and separation of organic mixtures (Delanaye et al., 2006; Duarte, Bordado, & Cidade, 2007; Ismail & Hassan, 2004; Kalocheretis et al., 2006).

This work shows the potential use of cellulose from mango seeds and newspaper to produce CA asymmetric membranes. CA was characterized by FTIR, determination of the degree of substitution (DS), viscosity average molecular weight (M_v), themogravimetric analysis (TGA), differential scanning calorimetry (DSC) and X-ray diffraction. Membranes were produced by the phase inversion technique using different formulations of a CA/dichloromethane/water solution, with and without the use of magnesium perchlorate, and were evaluated by thermal analysis (TGA and DSC), scanning electron microscopy (MEV), water vapor flux and ion diffusion.

2. Experimental

2.1. Delignification of newspaper

Only parts without ink were used. Newspaper was shredded and the delignification was carried out as described by Rodrigues Filho et al. (2000): 4.000 g of newspaper was mixed with 76.00 mL water. After 24 h, the mixture was filtered and 76.00 mL NaOH (0.25 mol L^{-1}) was added to the newspaper. After 18 h, the mixture was filtered again and the newspaper put into reflux with three successive portions of a 20% v/v mixture of nitric acid and ethanol, which was changed after each hour. After the reflux, the mixture was filtered, and then washed with distilled water until the filtrate became uncolored. The newspaper was dried at 105 °C for 180 min and then ground.

2.2. Treatment of mango seed with NaOH

Mango seed integument (1.000 g), previously washed to remove the fruit pulp, dried and ground, was immersed in NaOH 1 M for 24 h. Then, the mixture was filtered, washed with distilled water and neutralized with acetic acid 10% v/v. The material was dried in an oven at 90 °C for 3 h and stored for posterior use.

The content of Klason lignin for both materials, mango seed and newspaper was determined as described elsewhere (Vieira et al., 2007) for each material.

2.3. Synthesis of cellulose acetate

A mixture composed of 2.000 g cellulose (from newspaper or mango seed) and 50 mL acetic acid was stirred for 30 min at room temperature. Then, 0.32 mL H_2SO_4 and 18 mL acetic acid was added to the system, which was stirred for 25 min. The mixture was filtered and 64 mL acetic anhydride was added to the filtrate. This solution was returned to the recipient containing cellulose and stirred for 30 min. After this time, the mixture stood for 14 h at room temperature. Then, this mixture was vacuum filtered to remove undissolved particles and water was added to the filtrate to stop the reaction and precipitate CA, which was filtered, washed with distilled water to remove acetic acid and dried at 70 °C for 2 h (Cerqueira, Rodrigues Filho, & Meireles, 2007; Cerqueira, Valente, Rodrigues Filho, & Burrows, 2009). From now on, the materials will be called as CA-MN for cellulose acetate from mango seed and CA-NP for cellulose acetate from newspaper. The degree of substitution of the produced materials was determined by a saponification reaction (Rodrigues Filho et al., 2000) and the molecular weight was calculated by viscometry using the single point methodology (Cerqueira et al., 2007). The solvent used for the measurements of viscosity was the system dichloromethane/ethanol (8/2 v/v) for which $k = 13.9 \times 10^{-3}$ mL g^{-1} and $a = 0.834$ and the viscosity average molecular weight was determined according to the Mark–Houwink–Sakurada equation (Eq. (1)).

$$[\eta] = kM_v^a \tag{1}$$

where $[\eta]$ is the intrinsic viscosity; M_v is the viscosity average molecular weight; k and a are the constants related to the solvent.

2.4. FTIR spectroscopy

The experiments were carried out using a Shimadzu IRPrestige-21 equipment with step size of 4 cm^{-1}. Twenty scans were collected using KBr pellets (1/100 (w/w)).

2.5. X-ray diffractometry

X-ray diffraction patterns were obtained using a XRD-6000 Shimadzu with Cu Kα radiation from 5° to 50°.

2.6. Production of CA membranes

The membranes were produced using a modification of the methodology described by Khulbe et al. (2001): solutions containing CA, dichloromethane (CH_2Cl_2) and water with and without magnesium perchlorate ($Mg(ClO_4)_2$) were prepared in the proportions (w/w) shown in Table 1. Each mixture was stirred for 24 h in order to dissolve completely, and then, cooled down to 4 °C. The solution was cast on a glass plate, using a casting knife set at 400 μm at room temperature (28 °C). After one minute, the system was immersed in a water bath at 4 °C for 2 h. The membrane was removed and then dipped into a water bath at 85 °C for 10 min.

2.7. DSC and TGA experiments

DSC experiments were performed in a Q-20, TA Instruments, using sealed aluminum crucibles containing 10 mg of the samples. The heating rate was 10 °C min^{-1} and nitrogen flow was 50 cm^3 min^{-1}.

Table 1
Formulations utilized for preparing the membranes.

Material	CA (%)	CH_2Cl_2 (%)	Water (%)	$Mg(ClO_4)_2$ (%)
M-NP 1	9.28	83.48	6.49	0.74
M-NP 2	9.28	84.22	6.49	–
M-MG 1	7.5	86.59	5.29	0.60
M-MG 2	7.5	83.19	5.27	–

TGA experiments were performed in a TGA-50, Shimadzu. Ten milligram of the samples were heated from room temperature to 700 °C at a rate of 10 °C min^{-1} under nitrogen atmosphere.

2.7.1. SEM

Films were fractured in liquid nitrogen and fixed on a metal stub with double-sided adhesive tape. The cross-section and surface of the membranes were initially gold coated and the microscopies were obtained in a Shimadzu SSX-550 SuperScan, operated at 10 kV.

2.7.2. Water vapor flux

The water vapor flux through the membranes was measured using the Payne's cup technique (Rodrigues Filho et al., 2000). The membrane was cut into the shape of a disk, with the same diameter of the Payne's cup and had its thickness previously measured with a micrometer. Water was added to the cup and the disk was placed onto the cup's support. The system was weighed and put into a desiccator, and was weighed at every hour, for 9 h, which was sufficient for reaching the steady-state regimen. Weight-loss was calculated according to Eq. (2).

$$J = \frac{\Delta m}{\Delta t} A \tag{2}$$

where J = water vapor flux; Δm = mass difference; Δt = time difference; A = membrane area.

2.7.3. Diffusion of ions

For these experiments, it was used a two-compartment system separated by the studied membrane. One of the compartments was filled with deionized water, and the other with KCl solution (10^{-3} mol L^{-1}). A calibration curve was built, by measuring the conductivity of several concentrations of KCl solutions. This curve was posteriorly used to calculate the concentrations of KCl during the diffusion experiments. From the slope of the concentration in function of time, the flow (J) through the membrane was calculated. The permeability coefficient (P) was calculated from Eq. (3) (Meireles et al., 2008).

$$P = \frac{J}{\Delta C} \tag{3}$$

where ΔC is the concentration difference between the two compartments.

The ion diffusion coefficients (D) through the membranes were calculated using the Eq. (4).

$$D = Pd \tag{4}$$

where d is the membrane thickness.

3. Results and discussion

3.1. Characterization of the raw materials: Klason lignin and FTIR

The content of Klason lignin (insoluble in acid) in mango seed (raw and treated with NaOH) was 26.6 ± 1.0% and 24.5 ± 2.0%, respectively. Even though this treatment does not change the lignin content in the sample, it is necessary since it improves cellulose accessibility and favors the posterior chemical modification for producing CA.

Klason lignin in raw newspaper was determined as 24.65 ± 0.8%. Although this value is similar to the value found for treated mango seed, it was not possible to produce CA neither from raw newspaper nor from newspaper treated with sodium hydroxide. Thus, the newspaper needed a more aggressive treatment to reduce its lignin content to about 15.5 ± 2.0%. Press paper is produced from *Pinus*, which presents guaiacyl as predominant lignin. The high residual lignin content even after the delignification process is due to guaiacyl lignin, which is strongly bonded to the cellulose fibers.

The presence of residual lignin is also observed in the FTIR spectra in Fig. 1.

FTIR spectra present the typical pattern for lignocellulosic materials. Both spectra present absorption bands in the region attributed to functional groups that are present in fragments of lignin such: 1728 cm^{-1}, attributed to stretching of C=O groups, non-conjugated to the aromatic ring; 1515 cm^{-1} attributed to C—C stretching of aromatic rings in lignin; 1278 cm^{-1} and 810 cm^{-1}, attributed to C—O stretching of guaiacyl rings (Pandey & Pitman, 2003; Tejado, Peña, Labidi, Echeverria, & Mondragon, 2007).

In spite of the high lignin content in delignified newspaper and mango seed after NaOH treatment, it was possible to produce CA from both sources. Lignin had influence in the characteristics of the produced cellulose acetates and membranes.

3.2. Characterization of cellulose acetate

Fig. 2 shows the FTIR spectra of CA of both sources. The spectra preset the typical absorption bands of acetylated materials: in 1750 cm^{-1}, which is attributed to ester C=O stretching, in 1240 and 1050 cm^{-1}, which are related to C—O bond. It is also seen a reduction in the absorption intensity of the band in 3500 cm^{-1}, which is related to the axial vibration of the O—H bonds, in relation to non-acetylated materials (He, Zhang, Cui, & Wang, 2009; Mark, 1999). The spectra show that the materials were acetylated and the degrees of substitution determined through the chemical route were 2.65 ± 0.06 for CA-MG and 2.64 ± 0.07 for CA-NP.

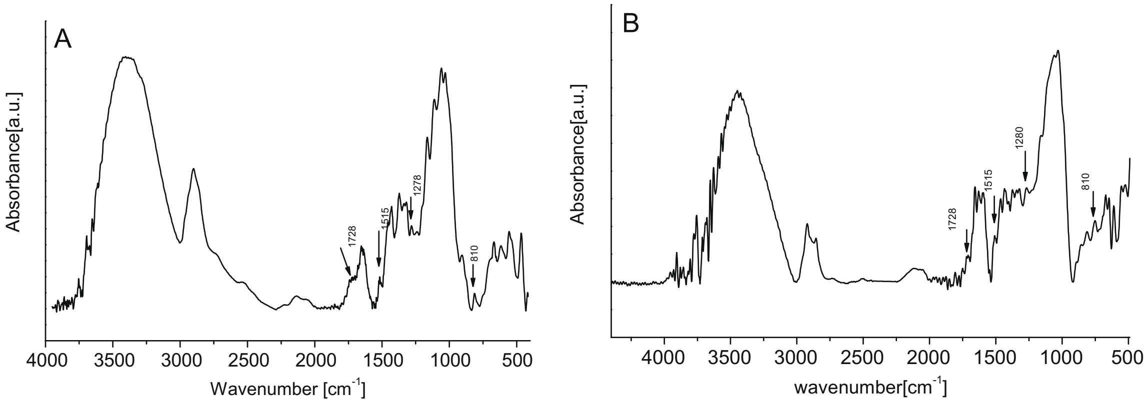

Fig. 1. FTIR spectra for delignified newspaper (A) and mango seed after NaOH treatment (B).

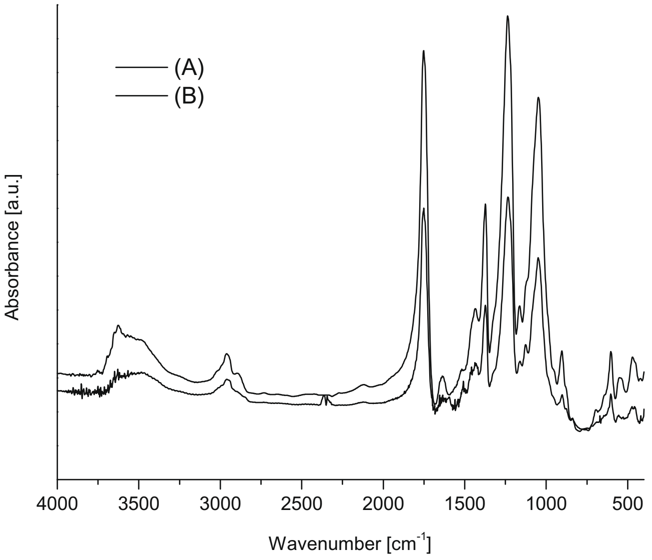

Fig. 2. FTIR spectra for powder cellulose acetates, CA-NP (A) and CA-MG (B).

3.3. Viscosity average molecular weight (M_v)

M_v was calculated by viscosity measurements for both materials and the values were 21,500 g mol^{-1} for CA-NP and 49,000 g mol^{-1} for CA-MG. Posterior results showed that the membrane morphology is influenced by CA molecular weight.

3.4. Thermal analysis: DSC and TGA

Fig. 3 shows the DSC and TGA curves for the produced CA samples, in powder form.

DSC thermogram of CA-NP shows an endotherm around 100 °C, which is attributed to water loss, an exotherm around 199 °C, which is attributed to the crystallization of the material and a second endotherm in 298 °C which is attributed to the degradation, since TGA curve presents weight loss in this same position.

DSC thermogram of CA-MG presents, besides the water loss endotherm around 100 °C, two other endotherms, one in 250 °C and other in 308 °C. The endotherm at 250 °C can be attributed to the degradation of acetates of both hemicelluloses and lignins, what is confirmed by the weight loss in its TGA curve (Ren, Sun, Liu, Cao, & Luo, 2007). The degradation temperature for acetylated hemicellulose is 230 °C, while lignin degrades from 190 to 900 °C. Shaikh, Pandare, Nair, and Varma (2009) also showed that acetylated hemicelluloses, such xylan acetate, present DSC endotherms at 215 °C and weight loss in 220 °C. The endotherm in 308 °C, starting at 290 °C, would be usually attributed to the fusion of CA, but this endotherm is related to weight loss, as observed by TGA. Therefore, this phenomenon is caused by the degradation of the CA chains.

Furthermore, even though CA-NP also presents lignin and hemicelluloses in its composition, some of those constituents are easily eliminated by hydrolysis and dissolution in the reaction medium during the acetylation process (Shaikh et al., 2009). This was confirmed by the determination of Klason lignin, in the produced CAs, from which CA-NP presented a lignin content of 4.0 ± 1.5% and CA-MG 13.0 ± 1.1%, what justifies the DSC patterns in which only CA-MG presents an endotherm around 250 °C.

3.5. X-ray diffraction (XRD)

Fig. 4 shows the X-ray difractograms for the produced CA samples. CA-NP presents a maximum at 8.0°, 17.6° and 21.7°, while CA-MG presents maxima at 8.2°, 10.1°, 12.9°, 17.1° and 21.9°. These diffraction patterns for both materials correspond to the structure of acetylated materials (Kono, Numata, Nagai, Erata, & Takai, 1999; Shaikh et al., 2009), being the halos at 8.0°, 10.0° and 22.0° the most important. The maximum at 8.0° is attributed to the generation of disorder when cellulose is acetylated. The maximum at 22.0° is called van der Walls halo and is present in all polymers and corresponds to the packing of the polymer chains due to the van der Walls forces (Rodrigues Filho et al., 2000). The halo in 10.0° is called larger than van der Walls halo and occurs for some amorphous polymers due to the existence of regions with aggregates of parallel chain segments (Miller & Boyer, 1984; Rodrigues Filho et al., 2000).

When comparing the CA XRD patterns with those obtained by Kono et al. (1999), it can be seen that the diffraction pattern obtained for CA-MG is similar to cellulose triacetate II (CTAII), while CA-NP presents CTAI structure, which is due to the predominant lignin, which is guaiacyl. This kind of lignin even after delignification is kept in the material, hampering the conversion from cellulose I to cellulose II, during the delignification process, for being strongly attached to the cellulose fibers. For mango seed cellulose, on the other hand, in which guaiacyl lignin is not predominant, only the mercerization process was enough for partial conversion from cellulose I to cellulose II, which was complete after acetylation, resulting into a diffraction pattern of CTA II, produced from cellulose II.

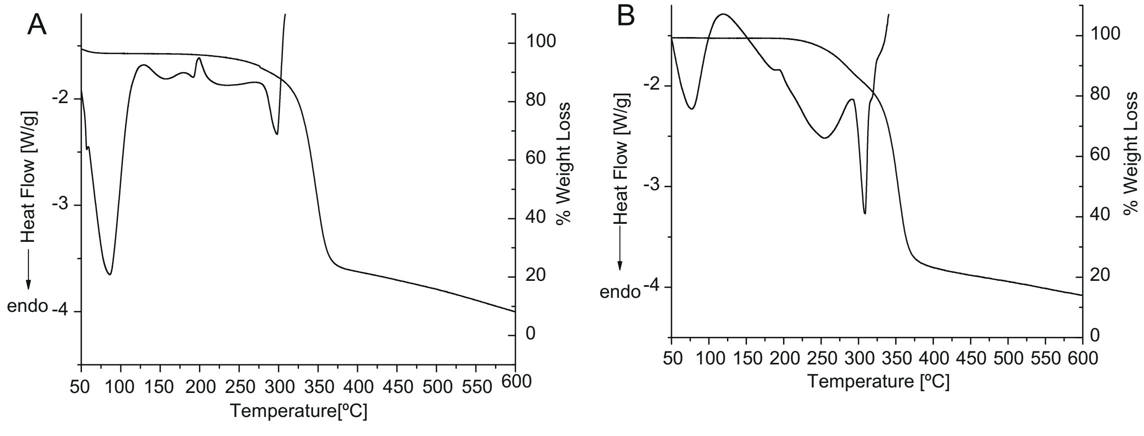

Fig. 3. DSC and TGA of cellulose acetate samples, in powder form. (A) CA-NP; (B) CA-MG.

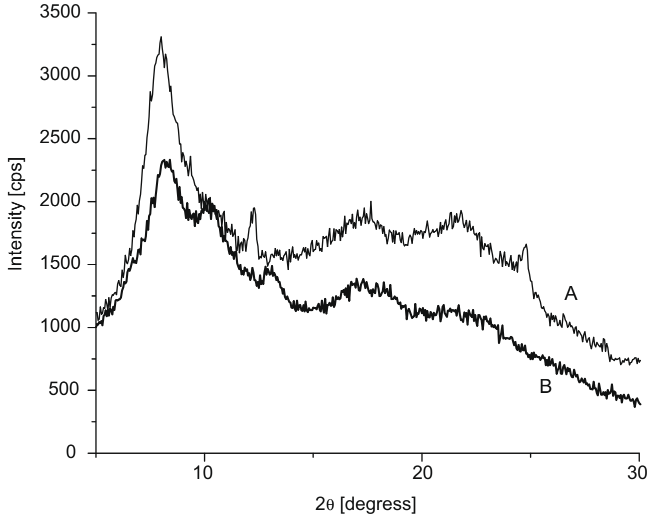

Fig. 4. XRD for powder materials: CA-NP (A) and CA-MG (B).

3.6. Characterization of CA membranes

3.6.1. DSC and TGA

Fig. 5 shows the DSC thermograms and TGA curves of the membranes. The DSC thermograms present an endotherm around 100 °C which is attributed to water loss, an exotherm around 199 °C attributed to the material crystallization and a second exotherm in 298 °C that is attributed to the fusion of the materials. However, as discussed for the DSC thermograms of the powder samples, these endotherms are accompanied by weight loss and are attributed to the degradation of cellulose acetate chains.

Concerning the thermal stability of the membranes, Fig. 5 shows that when magnesium perchlorate is added to the formulation there is no change in the profile of thermal degradation for the membranes produced with CA-NP, while for M-MG 1 the thermal stability was reduced in relation to M-MG 2. This profile of degradation is possibly related to the kind of structure formed in the precipitation of this membrane by the presence of salt with other components such as acetylated lignin and hemicelluloses in CA-MG.

3.6.2. SEM

Fig. 6 shows the scanning electron microscopy of both surfaces of the membranes, surface in contact with air and surface in contact with the substratum (glass plate).

It is observed that the produced membranes of both materials, without magnesium perchlorate in the composition is less porous in the interface in contact with air and with the substratum (glass) than those produced with salt. This morphology is according to that found by Khulbe et al. (2001), where magnesium perchlorate and water act as swelling agents in the membrane formation leading to pore formation. The salt addition in the tested formulations, CA/Dichloromethane/water and CA/Dichloromethane/water/salt, improved the solution stability, avoiding phase separation. As magnesium perchlorate leaves the membrane into the water bath, the system stabilizes and promotes a gradual phase inversion

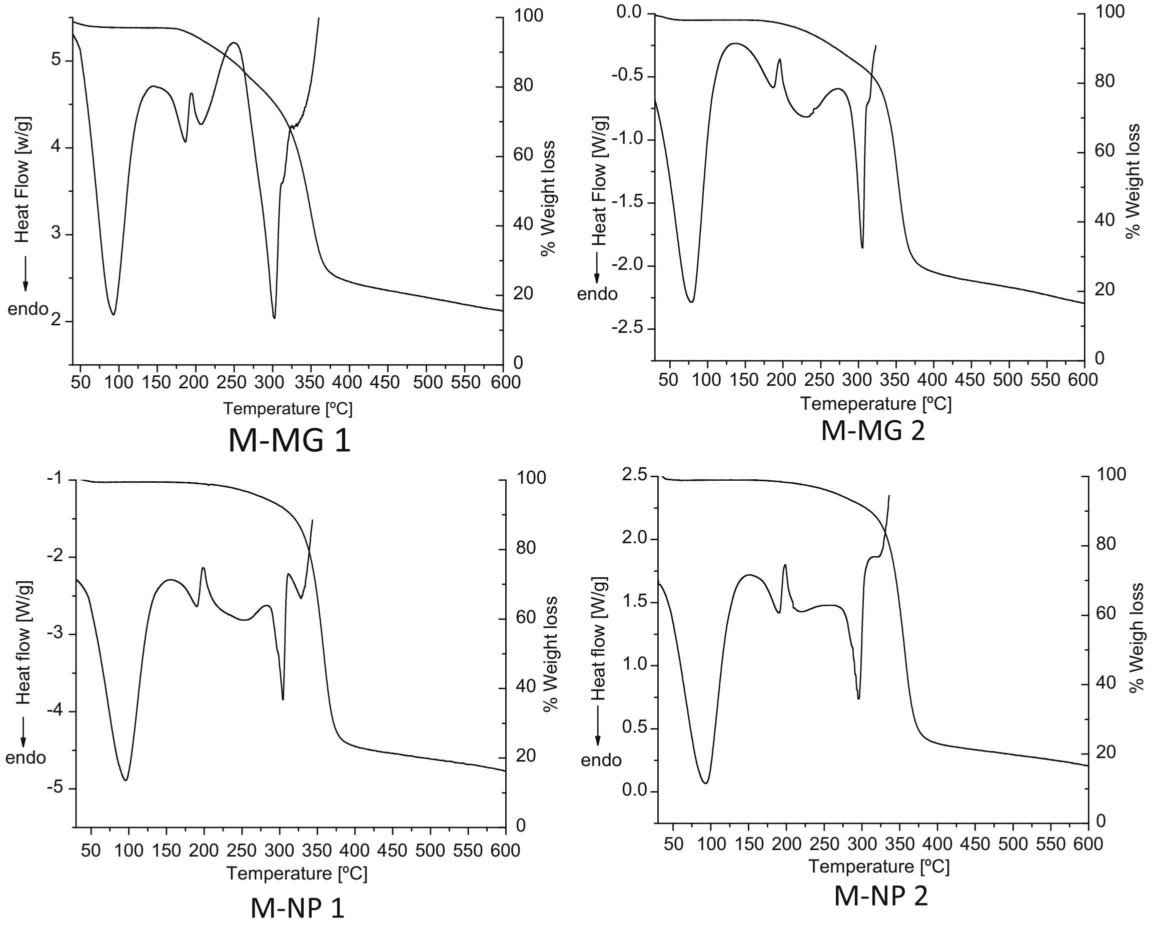

Fig. 5. DSC thermograms and TGA curves for distinct membrane formulations 1: with salt, 2 without salt.

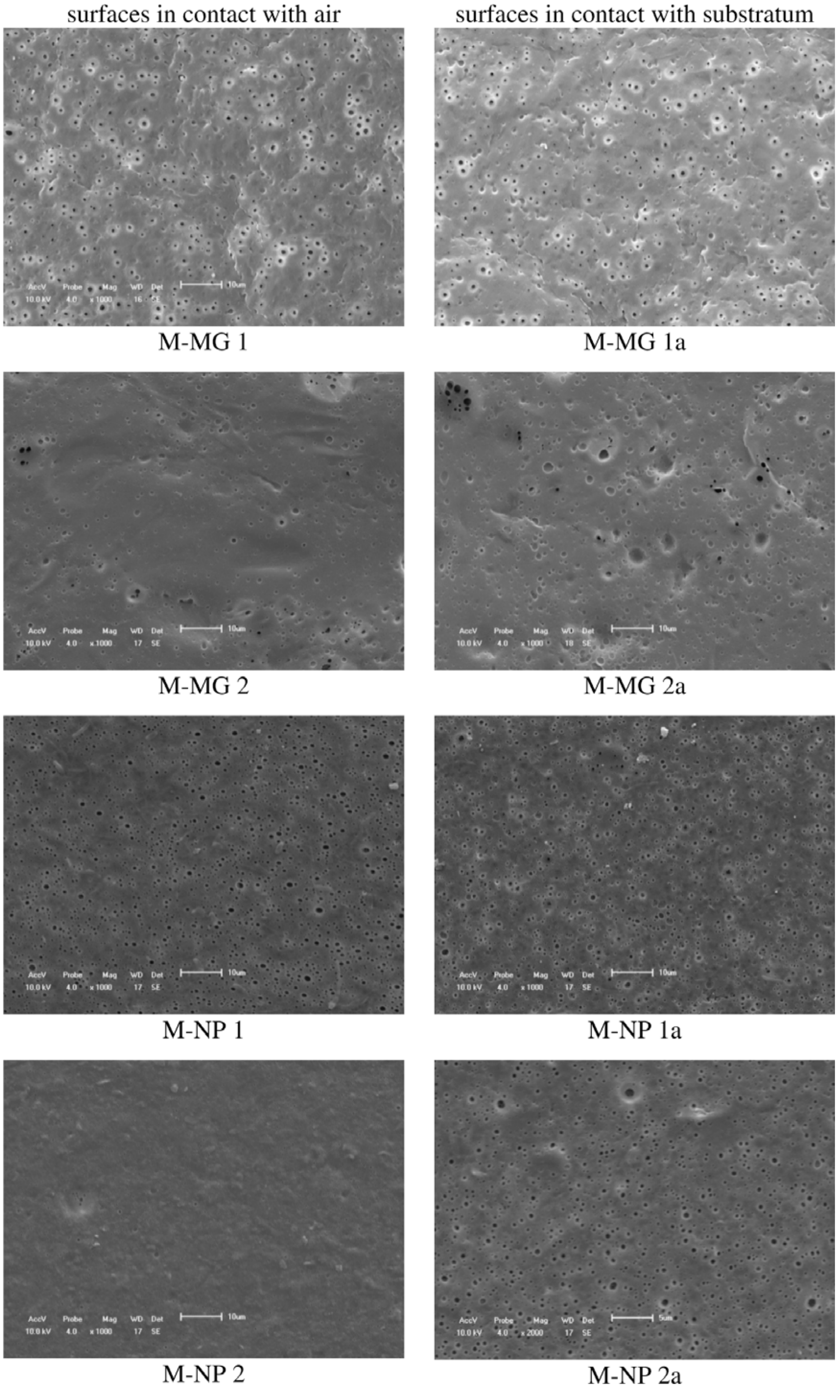
surfaces in contact with air

surfaces in contact with substratum

M-MG 1

M-MG 1a

M-MG 2

M-MG 2a

M-NP 1

M-NP 1a

M-NP 2

M-NP 2a

Fig. 6. SEM of the surfaces in contact with air (1: with salt and 2: without salt) and surfaces in contact with substratum (1a: with salt and 2a: without salt). Magnification of 1000×.

without a heterogeneous precipitation. In formulations without salt, there is a fast phase separation on the system, what results in more fragile membranes. Thus, salt addition has an important role for stabilizing CA/dichloromethane/water solution and is determinant on the final characteristics of the produced membranes.

Both molecular weight of the polymers and the lignin content in CAs have influence on the structure formation. In order to discuss the influence of lignin, M-MG 2 and CA-NP 2 will be used as examples. M-MG 2 presents pores even without salt in its formulation, due to the presence of lignin fragments, which affect the interactions between the polymer chains, resulting in low density regions in the polymer. Thus, pore formation is favored in M-MG even without addition of magnesium perchlorate, when compared with the membranes produced from CA-NP, due to its lower lignin content (as discussed previously by the determination of Klason lignin for CAs).

Fig. 7 shows the cross-section of the membranes CA-MG and CA-NP with and without salt as an example of the molecular weight influence in the morphology of the membranes.

Firstly, an asymmetric structure is observed in each of the membranes. The cross-sections of the membranes produced from CA-MG present regions of high density, opposite to what is observed for membranes produced from CA-NP. The regions with

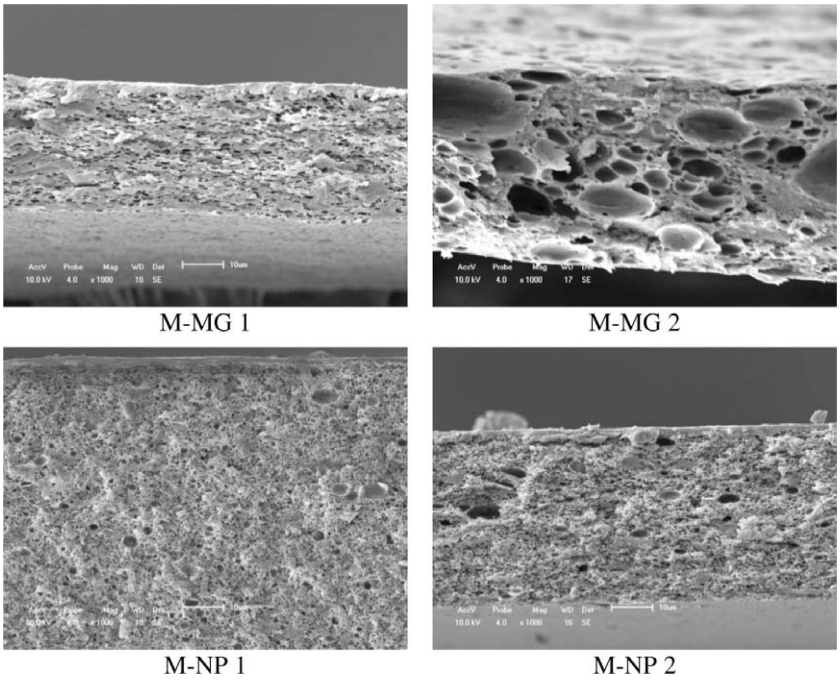

M-MG 1 M-MG 2

M-NP 1 M-NP 2

Fig. 7. Cross-sections of the M-MG 1 and M-MG 2, CA-NP 1 and CA-NP 2, magnified 1000×.

higher polymer density are produced by the influence of the higher molecular weight, where the presence of longer polymer chains increase the interactions between the chains. The formation of the substructure morphology of the membrane is then a competition between the influences of the lignin content and polymer molecular weight.

3.6.3. Transport property: Water vapor flow and ion diffusion

The water vapor flux through the produced membranes are: 0.85×10^{-4} g s^{-1} cm^{-2} μm and 1.02×10^{-4} g s^{-1} cm^{-2} μm for the M-MG 1 and M-NP 1, respectively, and 3.11×10^{-5} g s^{-1} cm^{-2} μm and 7.30×10^{-5} g s^{-1} cm^{-2}μm for the M-MG 2 and M-NP 2, respectively. Membranes produced with magnesium perchlorate in their composition presented higher values of water vapor flux since the membrane superficial layer becomes more porous, as observed by SEM, in Fig. 7 (M-MG 1 and M-NP 1). The superficial layer is determinant in the water vapor transport, since when membranes CA-NP 1 and CA-MG 1, which have a porous superficial layer, are compared the values found of water vapor flux are very similar.

On the other hand, comparing the ion diffusion results, the value found for the diffusion coefficient was 1.82×10^{-8} cm^2 s^{-1} for M-MG 1 and 7.43×10^{-8} cm^2 s^{-1} for M-NP 1, i.e., the ion diffusion coefficient of M-MG 1 is four times lower. This difference can be also explained by the difference in the substructure morphology, as the high density regions in CA-MG 1 membranes hamper the ion diffusion through these membranes. On the other hand, CA-NP 1 membranes, which present smoother morphology, presents its flux facilitated, and its value is similar to commercial CA membranes, 8.47×10^{-8} cm^2 s^{-1} (Meireles et al., 2008), demonstrating the potential of newspaper for this purpose. M-MG 2 and M-NP 2, were too fragile and it was not possible to carry out ion diffusion experiments with them. Even though M-NP 1 presented better performance in the ion diffusion experiment, it allowed water flow even before the start of resistance to pressure with water permeation experiment and broke just after its start, demonstrating its fragility for experiments dealing with difference of pressure. On the other hand, M-MG 1 resisted up to 1.5 atm. This difference in the resistance of the membranes might be connected to the presence of acetylated hemicelluloses, such as xylan acetate, which, according to Shaikh et al. (2009) act as plasticizer and can improve the mechanical properties of these materials.

4. Conclusion

Results showed that with the utilized compositions, CA/dichloromethane/water and CA/dichloromethane/water/magnesium perchlorate it was possible to produce asymmetric membranes from CA produced from mango seed and newspaper. Results with the different raw material sources were different in relation to the characterization of the produced CAs, as for example, the viscosity average molecular weight (21,500 g mol^{-1} for CA-NP and 49,000 for CA-MG). Regarding XRD, results showed diffraction patterns similar to CTA I and CTA II for CA-NP and CA-MG, respectively. Results of water vapor through the membranes showed that the superficial layer of the membranes is determinant for the water flow, since the membranes with a porous superficial layer, CA-NP and CA-MG with salt, presented higher flow. For the ion diffusion experiments, the membrane substructure was determinant, since the membrane with high density regions in its substructure, CA-MG, presented the lower ion diffusion coefficient. Magnesium perchlorate has an important role in the stability of the CA/dichloromethane/water solution and is determinant in the production of the membranes. The value of the ion diffusion coefficient for CA-NP is similar to the value reported in the literature for a commercial CA, 8.47×10^{-8} cm^2 s^{-1}, showing the potential of this membrane obtained from a recycled material for this purpose.

Acknowledgements

The authors acknowledge to CNPq for project Casadinho UFU/UFG/UFMS (620181/2006-0), to CAPES for the access to "Portal Periódicos", to Finep/Sebrae for project 0535/07 ref 3119/06. Meireles thanks CAPES for her PhD scholarship, Ribeiro thanks FAPEMIG for the scholarships related to projects PIBIC A-025/2008 and CEX – APQ-00466-08.

References

Ajila, C. M., Bhat, S. G., & Rao, U. J. S. P. (2007). Valuable components of raw and ripe peels from two Indian mango varieties. *Food Chemistry, 102*(4), 1006–1011.

Borges, C. A. M., Siqueira, D. L., Dias, D. C. F. S., & Cardoso, A. A. (1999). Caracterização e correlações biométricas de sementes das mangueiras 'espada' e 'ubá'. *Revista Ceres, 46*, 219–229.

Cerqueira, D. A., Rodrigues Filho, G., & Meireles, C. S. (2007). Optimization of sugarcane bagasse cellulose acetylation. *Carbohydrate Polymers, 69*(3), 579–582.

Cerqueira, D. A., Valente, A. J. M., Rodrigues Filho, G., & Burrows, H. D. (2009). Synthesis and properties of polyaniline–cellulose acetate blends: The use of sugarcane bagasse waste and the effect of the substitution degree. *Carbohydrate Polymers, 78*(3), 402–408.

Chou, W. L., Yu, D. G., Yang, M. C., & Jou, C. H. (2007). Effect of molecular weight and concentration of PEG additives on morphology and permeation performance of cellulose acetate hollow fibers. *Separation and Purification Technology, 57*(2), 209–219.

Delanaye, P., Lambermont, B., Dogne, J. M., Dubois, B., Ghuysen, A., Janssen, N., et al. (2006). Confirmation of high cytokine clearance by hemofiltration with a cellulose triacetate membrane with large pores: An in vivo study. *International Journal of Artificial Organs, 29*(10), 944–948.

Duarte, A. P., Bordado, J. C., & Cidade, M. T. (2007). Cellulose acetate reverse osmosis membranes: Optimization of preparation parameters. *Journal of Applied Polymer Science, 103*(1), 134–139.

Habert, A. C., Borges, C. P., & Nobrega, R. (2006). *Processos de separação por membranas*. Rio de Janeiro: E-papers.

He, J., Zhang, M., Cui, S., & Wang, S.-Y. (2009). High-quality cellulose triacetate prepared from bamboo dissolving pulp. *Journal of Applied polymer science, 113*, 456–465.

Ismail, A. F., & Hassan, A. R. (2004). The deduction of fine structural details of asymmetric nanofiltration membranes using theoretical models. *Journal of Membrane Science, 231*(1–2), 25–36.

Kalocheretis, P., Vlamis, I., Belesi, C., Makriniotou, I., Zerbala, S., Savidou, E., et al. (2006). Residual blood loss in single use dialyzers: Effect of different membranes and flux. *International Journal of Artificial Organs, 29*(3), 286–292.

Khulbe, K. C., Matsuura, T., Lamarche, G., Lamarche, A. M., Choi, C., & Noh, S. H. (2001). Study of the structure of asymmetric cellulose acetate membranes for reverse osmosis using electron spin resonance (ESR) method. *Polymer, 42*(15), 6479–6484.

Kono, H., Numata, Y., Nagai, N., Erata, T., & Takai, M. (1999). CPMAS 13C NMR and X-ray studies of cellooligosaccharide acetates as a model for cellulose triacetate. *Journal of Applied Polymer Science. Part A: Polymer Chemistry, 37*, 4100–4107.

Mark, J. E. (1999). *Polymer data handbook*. Oxford: Oxford University press.

Meireles, C. S., Rodrigues Filho, G., Assunção, R. M. N., Cerqueira, D. A., Zeni, M., Mello, K., et al. (2008). Production and characterization of membranes of recycled waste materials: Cellulose acetate, obtained from sugarcane bagasse with polystyrene from plastics cups. *Polymer Engineering and Science, 48*(8), 1443–1448.

Miller, R. L., & Boyer, R. F. (1984). X-Ray scattering from amorphous acrylate and methacrylate polymers: Evidence of local order. *Journal of Polymer Science, 22*, 2021–2041.

Olle, D., Lozano, Y. F., & Brillouet, J. M. (1996). Isolation and characterization of soluble polysaccharides and insoluble cell wall material of the pulp from four mango (*Mangifera indica* L.) cultivars. *Journal of Agricultural and Food Chemistry, 44*(9), 2658–2662.

Pandey, K. K., & Pitman, A. J. (2003). FTIR studies of the changes in wood chemistry following decay by brown-rot and white-rot fungi. *International Biodeterioration & Biodegradation, 52*(3), 151–160.

Ren, J. L., Sun, R. C., Liu, C. F., Cao, Z. N., & Luo, W. (2007). Acetylation of wheat straw hemicelluloses in ionic liquid using iodine as a catalyst. *Carbohydrate Polymers, 70*(4), 406–414.

Rodrigues Filho, G., Cerqueira, D. A., Assunção, R. M. N., Meireles, C. S., & Valente, A. (2008a). Recycling of sugarcane bagasse for producing cellulose acetate. *Polymers Research Journal, 1*, 243–252.

Rodrigues Filho, G., da Cruz, S. F., Pasquini, D., Cerqueira, D. A., Prado, V. D., & Assuncao, R. M. N. (2000). Water flux through cellulose triacetate films produced from heterogeneous acetylation of sugar cane bagasse. *Journal of Membrane Science, 177*(1–2), 225–231.

Rodrigues Filho, G., Monteiro, D. S., Meireles, C. S., Assuncao, R. M. N., Cerqueira, D. A., Barud, H. S., et al. (2008b). Synthesis and characterization of cellulose acetate produced from recycled newspaper. *Carbohydrate Polymers, 73*(1), 74–82.

Shaikh, H. M., Pandare, K. V., Nair, G., & Varma, A. J. (2009). Utilization of sugarcane bagasse cellulose for producing cellulose acetates: Novel use of residual hemicellulose as plasticizer. *Carbohydrate Polymers, 76*(1), 23–29.

Sossna, M., Hollas, M., Schaper, J., & Scheper, T. (2007). Structural development of asymmetric cellulose acetate microfiltration membranes prepared by a single-layer dry-casting method. *Journal of Membrane Science, 289*(1–2), 7–14.

Tejado, A., Peña, C., Labidi, J., Echeverria, J. M., & Mondragon, I. (2007). Physico-chemical characterization of lignins from different sources for use in phenol–formaldehyde resin synthesis. *Bioresource Technology, 98*(8), 1655–1663.

Velan, M., Krishnan, M. R. V., & Lakshmanan, C. M. (1995). Conversion of mango kernel starch to glucose syrups by enzymatic-hydrolysis. *Bioprocess Engineering, 12*(6), 323–326.

Vieira, R. G. P., Rodrigues Filho, G., Assunção, R. M. N., Meireles, C. S., Vieira, J. G., & de Oliveira, G. S. (2007). Synthesis and characterization of methylcellulose from sugar cane bagasse cellulose. *Carbohydrate Polymers, 67*(2), 182–189.